Novel iGluSnFR3 variants with improved kinetics and dynamic range for tracking high frequency firing at glutamatergic synapses

Oanh Tran[1], Sara Bertelli[2], Holly J. Hughes[1], Luka Lozo[1], Andrew Plested[2], Katalin Török[1*]

[1]Neuroscience and Cell Biology Research Institute, City St George's, University of London, London, UK; [2]Humboldt University Berlin & Cluster of Excellence NeuroCure, Berlin, Germany

*** Correspondence:**
Katalin Török
k.torok@sgul.ac.uk

Keywords: biosensor, glutamate, neurotransmission, fluorescence

Abstract

The first genetically encoded single fluorescent protein-based glutamate sensor, iGluSnFR opened a new era of imaging neuronal activity at the level of circuits as well as at synapses. With slow *off*-kinetics, iGluSnFR could only resolve low frequency glutamate release. A binding site variant of iGluSnFR, $iGlu_u$ with significantly faster *off*-kinetics, enabled the resolution of high (100 Hz) frequency glutamate release in hippocampal slices at individual CA3-CA1 synapses. Moreover, $iGlu_u$ revealed impairment of glutamate retrieval in HD mice models pointing to defective glutamate transport. Recently, the iGluSnFR3 generation (SF-Venus-iGluSnFR. v857) has been developed with increased dynamic range and rapid *on*-kinetics, making it attractive for *in vivo* imaging. However, similarly to iGluSnFR, glutamate *off*-kinetics of iGluSnFR3 were predicted to limit it to resolving low frequency release only. We undertook to improve the kinetic properties of iGluSnFR3 for resolving high (100 Hz) frequency glutamate release. We generated and characterized iGlu3fast, an ultrafast decay variant of iGluSnFR3. For iGlu3Fast we obtained a decay rate constant of 340 ± 48 s^{-1}, ~5-fold faster than iGluSnFR3 at 71 ± 3 s^{-1}, at 20ºC. Furthermore, iGlu3Fast superseded iGluSnFR3 with a 42-fold glutamate-induced fluorescence increase compared to 26 for iGluSnFR3. Thus, with rapid *off*-kinetics comparable to that of $iGlu_u$ as well as significantly increased fluorescence dynamic range and preserved rapid *on*-kinetics, iGlu3fast represents an excellent novel sensor for imaging high frequency glutamate release at all levels of organisation. Two novel variants with superslow *off*-kinetics are also reported, expanding the range of applications in neurobiology.

Introduction

A direct way to image neural activity is by monitoring neurotransmitter release at the synapses. With glutamate being the most abundant excitatory neurotransmitter in the CNS, development of a fluorescent glutamate indictor has long been the aim of researchers. The first genetically encoded single fluorescent protein-based glutamate sensor, iGluSnFR opened a new era for imaging of neuronal activity at potentially all levels of organization (1). The design of iGluSnFR mimicked that of other cpEGFP-based approaches, however rather than binding two components e.g. CaM and RS20 peptide, it had the N and C-terminal portions of GluBP fused

to each terminus of cpEGFP (**Figure 1&2A**). Glutamate binding reconstituted GluBP, in turn correcting the cpEGFP defect. In terms of mechanism, initial glutamate binding to iGluSnFR does not affect the fluorescence intensity which then increases in the subsequent conformational change, the rate limiting step in the fluorescence response (**Figure 1**) (2). The *off*-kinetics of iGluSnFR, while it represented a milestone in terms of imaging neurotransmitter release, was fast enough only to resolve low frequency glutamate release. A binding site variant of iGluSnFR, $iGlu_u$ with significantly faster *off*-kinetics, enabled the resolution of high (100 Hz) frequency glutamate release in hippocampal slices at individual C3-C1 synapses (2). Moreover, $iGlu_u$ revealed impairment of glutamate retrieval in HD mice models pointing to EAAT2 function defect (3). We furthermore generated binding site variants that improved the kinetics and/or reduced the affinity of iGluSnFR (4).

Recently, a new generation of genetically encoded glutamate sensors, iGluSnFR3 has been developed reporting increased dynamic range and rapid response kinetics, making its application attractive for *in vivo* imaging (5). iGluSnFR3 has the same domain structure as iGluSnFR with PDGFR or other membrane targeting motifs (**Figure 2A**). iGluSnFR3 is the v857 variant of SF-Venus-based iGluSnFR that was developed by high throughput technology incorporating several mutations and selected for having the best fluorescence and kinetic properties (5). However, similarly to iGluSnFR, glutamate *off*-kinetics of iGluSnFR3 limit it to resolving low frequency release patterns only. Given the distinct advantages of a rapid response sensor like $iGlu_u$ for resolving high (100 Hz) frequency glutamate release (2), we undertook to improve the kinetic properties of iGluSnFR3. We generated an ultrafast variant of iGluSnFR3 while also increasing its fluorescence dynamic range. We furthermore generated two variants with super-slow *off*-kinetics offering further tools for neurobiological investigations.

Materials and Methods

pRSET iGluSnFR3 v857 plasmid was a gift from Kaspar Podgorski (Addgene plasmid # 175186; http://n2t.net/addgene:175186; RRID: Addgene_175186). *E. coli* XL10-Gold and BL21 (DE3) Gold cells were purchased from Invitrogen.

Site-directed mutagenesis

Q5® Site-Directed Mutagenesis Kit (New England Biolabs) with the following primers (5' - 3') was used to generate iGluSnFR3 variants:

iGluSnFR3 S72T (iGlu3Fast), TCCGATTACTACGCAAAACCGTATTC

iGluSnFR3 D25A (iGlu3slow1), CGGTCACCGTGCCTCTTCAGTGC

iGluSnFR3 D25R (iGlu3slow2), CGGTCACCGTAGGTCTTCAGTGCC

DNA sequencing was carried out by Genewiz.

Protein expression and purification

iGlu3fast, iGlu3Slow1, iGlu3Slow2 and iGluSnFR3.v857 (iGluSnFR3) were overexpressed in *E. coli* B21 Gold cells using 0.5 mM isopropyl thio-β-D-galactoside (IPTG) and purified on a NiNTA column (QIAGEN, ÄKTA Purifier, GE Healthcare) at 4 °C as described previously (2). Protein was checked for purity by SDS-PAGE then stored at -80ºC.

Protein concentration measurements

Protein concentration was calculated from the absorption spectra of the proteins at 280 nm using the molar extinction coefficient of 52830 M^{-1} cm^{-1} calculated using the ProtParam tool (Expasy).

Equilibrium binding titrations

Fluorescence emission spectra were recorded using a Flurolog-3 spectrofluorimeter (Horiba©) at excitation wavelengths of 495 nm and emission wavelengths of 518 nm, 20 °C. 250 nM iGlu3fast, iGlu3Slow1, iGlu3Slow2 were titrated and compared with iGluSnFR3 in PBS buffer, pH 7.4 by stepwise addition of a solution of 50 - 500 mM glutamate until no further changes in fluorescence emission intensity were observed. Experiments were done in triplicates. Data was corrected for dilution, normalized and expressed as mean ± S.E.M. K_d for L-glutamate, L-aspartate and L-glutamine (the ligand concentration at which half-maximum fluorescence intensity is achieved) was obtained by fitting the data to a single site binding equation using GraphPad Prism 9 software.

Stopped-flow fluorimetry

Glutamate association and dissociation rates were measured using a TgK Scientific KinetAsyst™ double-mixing stopped-flow apparatus in single mixing mode. The fluorescence was excited at 495 nm and emission was collected using a 530 nm cut-off filter. For glutamate association, 250 nM iGlu3fast, iGlu3Slow1, iGlu3Slow2 or iGluSnFR3 in PBS buffer, pH 7.4 was rapidly mixed with increasing concentrations of glutamate (from 100 – 500 mM stock solution of glutamate in PBS) at 20 ºC. For glutamate dissociation, 250 nM protein in PBS buffer containing 100 - 300 µM glutamate was rapidly mixed with 1 - 3 mM purified bacterial periplasmic glutamate binding protein (GluBP) at 20 ºC. Experiments were done at least in triplicates. Averaged data were fitted to a single exponential function using KinetAsyst software (TgK Scientific) to obtain association or dissociation rates. All concentrations given were concentrations in the mixing chamber.

pH sensitivity

The apparent p*K*a was determined for iGlu3fast and compared with iGluSnFR3, using a series of buffers. Depending on their respective pH buffering range, an appropriate buffer was used for the measurements (MES for pH 6-6.5, HEPES for pH 7-8, TRIS for pH 8.5-9 and CAPS for pH 10). The pH titrations were performed by recording fluorescence spectra in PBS only or PBS with saturating glutamate (30 mM) using 250 nM protein in 0.5 pH unit intervals at 20 ºC (Fluorolog-3, Horiba©). Excitation wavelength was set at 495 nm and emission spectra were run in the 500-600 nm range.

Quantum yield determination

Measurements were made to compare iGlu3fast with iGluSnFR3 and iGluSnFR. Protein concentration was adjusted such that the absorbance at the excitation wavelength (492 nm) was between 0.001 and 0.1. A series of dilutions was prepared in PBS buffer only or PBS buffer with saturating glutamate (30 mM) and the fluorescence spectra were recorded on a Fluorolog-3 spectrofluorimeter (Horiba Horiba©). GCaMP6f quantum yield measured in Ca^{2+} -saturated buffer was used as a reference ($\Phi_{+Ca2+} = 0.59$) (6). Data were plotted as integrated fluorescence

intensity as a function of absorbance and fitted to a linear regression(S). Quantum yields were obtained using the following equation: $\Phi_{protein} = \Phi_{GCaMP6f} \times (S_{protein}/S_{GCaMP6f})$.

Cell culture and transfection

HEK293T cells were grown in MEM supplemented with 6% FBS, penicillin, and streptomycin, and maintained at 37°C in a 5% CO_2, 100% humidity atmosphere. Cells were transfected using PEI in a 1:3 ratio (vol/vol; DNA/PEI) the day after seeding. The ratios for co-transfection were 1:1 for GluA2 and iGlu3fast or iGluSnFR3, with a total of 2 µg DNA (1 µg/µL for each construct) per 35 mm dish. After 6 hours of incubation, the reaction was stopped, and the cells were split and seeded on 10 mm polylysine-coated coverslips. Currents were recorded 24–48 hours after transfection, with cells incubated at 37°C.

Dose response curves for iGlu3fast and iGluSnFR3 expressed on HEK293T cells

The amplitude of the fluorescence response was determined by patch-clamp fluorometry. After obtaining whole-cell access, lifted cells were placed in front of a piezo-driven square barrel fast perfusion tool (7) and subjected to the application of different solutions for activation by glutamate. Whole-cell patch clamp and simultaneous imaging recordings were performed in 158 mM NaCl, 20 mM HEPES-Na^+ pH 7.4, 3 mM KCl and 1 mM $CaCl_2$ extracellular solution. The intracellular (pipette) solution contained 135 mM KCl, 20 mM KF, 20 mM HEPES-Na^+ pH 7.4, 3 mM NaCl, 1 mM $MgCl_2$, and 2 mM EGTA (8). Currents were acquired using an Axopatch 200B amplifier and the Axograph acquisition program (Axograph Scientific) via an Instrutech ITC-18 D-A interface (HEKA Elektronik). After whole-cell configuration was obtained, cells were held at −50 mV, and current traces were filtered at 5 kHz and digitized at 20 kHz. Pipettes were made using borosilicate glass with an outer diameter of 1.17 mm and had a series resistance (R_s) between 2 and 6 MΩ, while the cell capacitance was between 5 and 25 pF, as measured by the compensating circuit of the amplifier. The maximum accepted voltage-clamp error, calculated as $I_{max} * R_s$, was 10 mV. The protocol consisted of repeated episodes in which cells underwent 300 ms piezo-controlled jumps to glutamate-containing solutions. The dose-response analysis was performed by exposing cells to 1 µM, 10 µM, 100 µM, 500 µM, 1 mM, and 10 mM glutamate, applied in a sparse order. For imaging, fluorescence intensities in response to 488-nm excitation were recorded at a 200-Hz frame rate, without binning, on a Prime 95B CMOS camera (Photometrics). An X-Cite Fluorescence Lamp was used for blue light emission, and camera exposure was triggered in hardware directly from the digitizer. Images were recorded with MicroManager (9) and analyzed with Fiji (10). All data were analyzed with IgorPro9 and the Neuromatics plugin.

Results

iGlu3fast, an ultrafast-decay kinetic variant of iGluSnFR3

We generated the ultrafast variant iGluSnFR3 S72T (iGlu3Fast) (**Figure 2**) and here we present its *in vitro* characterisation and comparison with iGluSnFR3.

iGluSnFR3 is reported to have a 50-fold fluorescence enhancement upon glutamate binding and an estimated *off*-rate of 34 s^{-1}, in PBS at 20 °C (5). First, we measured the fluorescence dynamic ranges of iGluSnFR3 and the variants. The iGlu3Fast variant superseded iGluSnFR3 with a relative fluorescence value of 42 compared to 26 measured for iGluSnFR3 in our hands

(**Table 1**). Second, we compared the *off*-kinetics of iGlu3Fast with that of iGluSnFR3 using excess GluBP to trap the released glutamate. We measured 340 ± 48 s^{-1} and 71 ± 3 s^{-1} for the *off*-rate for iGlu3Fast and iGluSnFR3, respectively (**Figure 3A&B**). Glutamate concentration dependence of the *on*-kinetics of iGlu3Fast and iGluSnFR3 was determined (**Figure 3C&D**), plotted and fitted to a hyperbolic function that describes a two-step reaction in which rapid binding is followed by a conformational change (**Figure 3E&F**). As shown in Scheme 1, fluorescence enhancement occurs in the second step (**Figure 1**). Equilibrium binding constant for the first step as well as the forward and reverse rate constants for the second, isomerization step (K_1, k_{+2}, k_{-2}, respectively) are fitted to the equation that provides analytical solution for the mechanism (2). **Table 1** shows all the fitted parameter values for the reaction scheme. The rate limiting *on*-rate was best fit to 832 ± 148 s^{-1} and 1399 ± 43 s^{-1}, for iGlu3Fast and iGluSnFR3, respectively.

Dissociation constants (K_d) for glutamate binding to purified proteins were measured by equilibrium titration as 3.18 ± 0.05 mM for iGlu3Fast and 373 ± 3 μM for iGluSnFR3 (**Figure 3G**, **Table 1**). The K_d values calculated from the fitted rate constants are in good agreement with the measured K_d values (**Table 1**). Expressed extracellularly in HEK293T cells and assayed by patch-clamp photometry, both iGlu3Fast and iGluSnFR3 displayed increased affinities compared to that measured for the purified proteins in solution, as it has been previously reported for iGluSnFR and its variants (1,2,5). On HEK293T cells the K_d for glutamate of iGlu3Fast was reduced to 162 ± 50 μM. The K_d of iGluSnFR3 was 16.3 ± 4.1 μM (consistent with that previously reported (5)) (**Figure 3H**). In summary, iGlu3Fast has a greater dynamic range, ~5-fold faster *off*-rate and an 8.5-fold higher K_d for glutamate than iGluSnFR3 in solution and 10-fold higher K_d for glutamate when expressed extracellularly in HEK293T cells.

pH dependences of iGlu3Fast and iGluSnFR3 were similar with pK_A values in the 7-7.5 range (**Figure 4**). The selectivity patterns with respect to aspartate and glutamine were also similar for iGlu3Fast and iGluSnFR3 with glutamine being barely detectable and the dynamic range for aspartate >2-fold reduced (**Figure 5**, **Table 2**) and consistent with that previously reported for iGluSnFR3 (5).

Brightness and quantum yield measurements of iGlu3Fast

Brightness and quantum yield data have been reported for iGluSnFR3 (5), but not for iGluSnFR. We wanted to see how the iGlu3Fast variant performs in comparison with the above two sensors. First, we measured iGluSnFR and found that the increase in brightness was mostly accounted for by an ~7-fold increase in the extinction coefficient. In contrast, as reported for iGluSnFR3, both the extinction coefficient and the quantum yield increased upon glutamate binding (5). However, in our hands the Glu-free form had higher and the Glu-bound form had lower brightness than the previously reported values. Because of the low fluorescence of the apo-forms, it was challenging to measure both the extinction coefficient and the quantum yield accurately. Notably, we measured higher brightness for iGluSnFR than for iGluSnFR3. The greater dynamic range of iGluSnFR3 and the further increased dynamic range of iGlu3Fast derived from lower brightness of the Glu-free form rather than greater brightness of the Glu-bound form (**Table 3**).

Super slow-decay kinetic variants of iGluSnFR3

We identified two iGluSnFR3 variants, D25A (iGlu3slow1) and D25R (iGlu3slow2), which presented with increased affinity for glutamate and accordingly with significantly reduced *off*-

rates while maintaining excellent fluorescence dynamic ranges of 16 and 23, respectively (**Supplementary Table 1**). The *off*-rate for (iGlu3slow1) was 0.017 ± 0.0001 s^{-1} and that for (iGlu3slow2) was 0.023 ± 0.0003 s^{-1}, ~15000-fold slower that the S72T variant (**Supplementary Figure 1A&B**). Glutamate concentration dependence of the *on*-kinetics was fitted to a hyperbolic function revealed fast isomerization rates of 1260 ± 34 and 1485 ± 222, respectively (**Supplementary Figure 1C&F**, **Supplementary Table 1**). Dissociation constants (K_d) measured by equilibrium titration for iGlu3slow1 and iGlu3slow2 were 58 ± 1 μM and 204 ± 8 μM, respectively (**Supplementary Figure G**). Expressed on the surface of HEK293T cells and assayed by patch-clamp photometry, iGlu3slow1 and iGlu3slow2 presented decay half-times of 0.29 and 0.33 s, respectively, consistent with the generally observed increased affinity for glutamate when expressed in cells compared to the purified protein in solution (data not shown).

Discussion

The development of genetically encoded glutamate sensors pioneered by iGluSnFR (1), allows imaging neural activity by directly monitoring neurotransmission. The iGluSnFR3 generation represents a significant improvement in the fluorescence dynamic range, a faster response *on*-rate, however with limiting decay kinetics.

iGlu3Fast, the S72T variant of iGluSnFR3 has a 5-fold faster decay rate than iGluSnFR3 and comparable to that of $iGlu_u$, which was derived from iGluSnFR by the same mutation. In addition, the S72T mutation further increased the fluorescence dynamic range of iGluSnFR3 from 26 to 42-fold. The 3.8 mM K_d measured for iGlu3Fast in solution is reduced, as previously reported for iGluSnFR and its variants (1,2), to 162 μM when expressed on the plasma membrane of HEK293T cells. The lowered affinity of the variant is favourable for detecting high transient local glutamate concentrations, e.g. in the synaptic cleft. In contrast, the super-slow decay variants iGlu3slow1 and iGlu3slow2 offer stable signals for large range imaging.

The utility of iGlu3Fast with greater fluorescence dynamic range and faster kinetic responses requires imaging systems capable of taking advantage of the improved sensor properties.

Acknowledgements

This work was supported by BBSRC grant BB/S003894/1 to K.T. Tom Carter is thanked for his comments on the manuscript.

Figure legends

Figure 1. Two-step model of the kinetic mechanism of genetically encoded glutamate sensors. Cartoon diagram depicting the putative molecular transitions of iGlu3Fast and iGluSnFR3 variants to the fluorescent state. Key: GluBP 1-253 (light blue) and 254-279 (dark blue) fragments, cpSF-Venus (yellow), glutamate (orange).

Figure 2. iGlu3Fast design. (**A**) Domain structure and design of single fluorophore-based genetically encoded glutamate indicator iGluSnFR3 indicating the S72T mutation; cpSF-Venus (yellow), IgG kappa secretion tag (pink), hemagglutinin (HA) tag (purple), myc tag (grey) and a PDGFR transmembrane domain (brown); GluBP 1-253 and 254-279 fragments are in light and dark blue, respectively. (**B**) Crystal structure of GluBP (PDB 2VHA, adapted from Hu *et al*. (Hu et al., 2008)). Mutated residue S72 at the glutamate binding site is shown as green backbone. Bound glutamate is represented in orange space filling display.

Figure 3. Kinetics of glutamate binding by iGluSnFR3 and its fast decay variant (20°C). (**A&B)** Glutamate dissociation kinetics (**C&D**) Glutamate association kinetics of iGlu3Fast and iGluSnFR3. Stopped-flow records of iGlu3Fast and iGluSnFR3 reacting with the indicated concentrations of glutamate. Experimental data are overlaid with curves fitted to single exponentials; (**E&F**) Plot of observed association rates, $k_{obs(on)}$ of iGlu3Fast and iGluSnFR3 as a function of glutamate concentration; (**G&H**) Glutamate titrations *in situ*. iGlu3Fast and iGluSnFR3 were expressed in HEK293T cells and (**G**) titrated with glutamate, (**H**) glutamate dose-response curve was measured by patch-clamp photometry.

Figure 4. pH sensitivity and pK_a determination of (**A**) iGlu3Fast and iGluSnFR3 (**B**). Normalised fluorescence in the presence (-■-) and absence of 30 mM glutamate (-●-).

Figure 5. Ligand selectivity. Equilibrium titrations of (**A**) iGlu3Fast and (**B**) iGluSnFR3 with glutamate, aspartate and glutamine, as indicated, at 20 ºC.

Figure 6. Kinetics of glutamate binding by iGluSnFR3 super-slow decay variants iGlu3slow1 and iGlu3slow2 (20°C). Glutamate dissociation kinetics of (**A**) iGlu3slow1, and (**B**) iGlu3slow2 determined by stopped-flow fluorimetry. Experimental data are overlaid by curves fitted to single exponentials. Fluorescence changes are normalised to F_{max} of 1. Glutamate association kinetics of (**C**) iGlu3slow1 and (**D**) iGlu3slow2. Stopped-flow records shows reactions with the indicated concentrations of glutamate. Experimental data are overlaid with curves fitted to single exponentials; (**E&F**) Plot of observed association rates, $k_{obs(on)}$ of iGlu3slow1 and iGlu3slow2 as a function of glutamate concentration; (**G**) Glutamate titrations *in situ*. iGluSnFR3 and variants were titrated with glutamate.

Table 1. Kinetic parameters of iGluSnFR3 and variants

Variant	F_{rel}	K_d mM	k_{-2} s^{-1}	K_1 M^{-1}	k_{+2} s^{-1}	K_d (calc) μM
iGlu3Fast	42 ± 1	3.18 ± 0.051	304 ± 33	0.074 ± 0.035	832 ± 147	3620
iGluSnFR3	26 ± 1	0.373 ± 0.003	71 ± 3	0.111 ± 0.011	1399 ± 43	398

k_{+2}, k_{-2} and K_1 are fitted values to Scheme 1. [a]Measured *off*-rates were used as constrains on hyperbolic fit. K_d was measured by equilibrium binding. [b]K_d (calc) is the value calculated from the fitted kinetic constants.

Table 2. Ligand selectivity of iGlu3Fast and iGluSnFR3

	Aspartate		Glutamine		Glutamate	
	F_r	K_d (μM)	F_r	K_d (μM)	F_r	K_d (μM)
iGlu3Fast	14.7 ± 0.2	112 ± 8	1.2 ± 0.1	53 ± 122	44.8 ± 0.2	2891 ± 64
iGluSnFR3	12.8 ± 0.3	223 ± 28	1.2 ± 0.1	79 ± 142	27.1 ± 0.1	348 ± 7

Table 3. Brightness measurements for iGlu3Fast, iGluSnFR3 and iGluSnFR

Variant	**iGlu3Fast**		**iGluSnFR3**		**iGluSnFR**	
	- Glu	**+ Glu**	**- Glu**	**+ Glu**	**- Glu**	**+ Glu**
ε_0(492 nm) $M^{-1}cm^{-1}$	1092.7	17858.0	6098.8	13794.5	9362.2	71912.8
ϕ	0.52	0.95	0.13	0.93	0.41	0.39
Brightness $mM^{-1}cm^{-1}$	0.570	17.1	0.784	12.8	3.8	27.9
Fold increase	1	30	1	16	1	7
ε_0(492 nm) $M^{-1}cm^{-1}$			[a]2000	[a]40000		
ϕ			[a]0.26	[a]0.93		
Brightness $mM^{-1}cm^{-1}$			[a]0.52	[a]37.2		
Fold increase			[a]1	[a]71.5		

[a]Aggarwal et al., 2023

Figure 1.

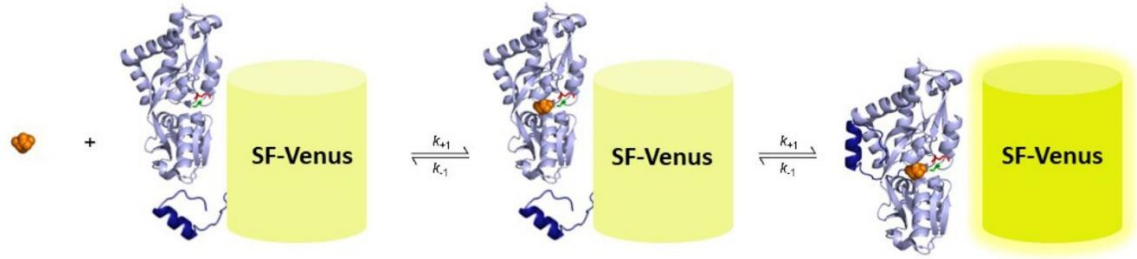

Figure 2.

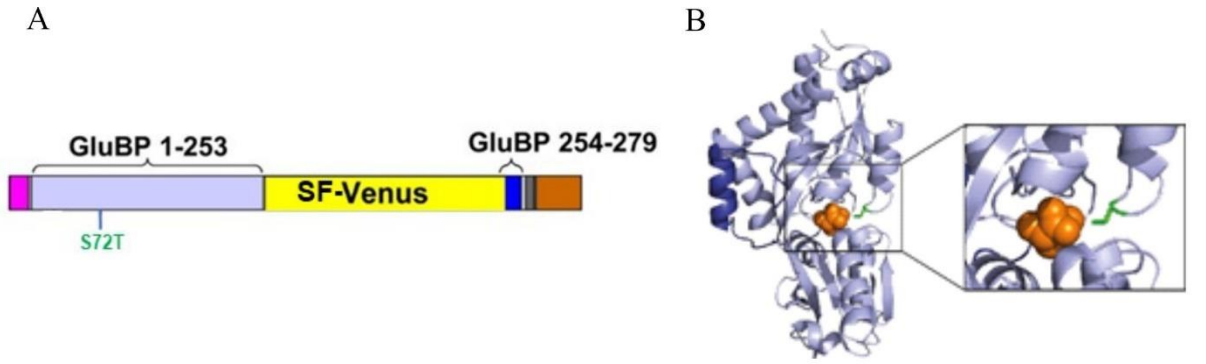

GluBP (PDB: 2VHA) (Hu *et al*., 2008)

Figure 3.

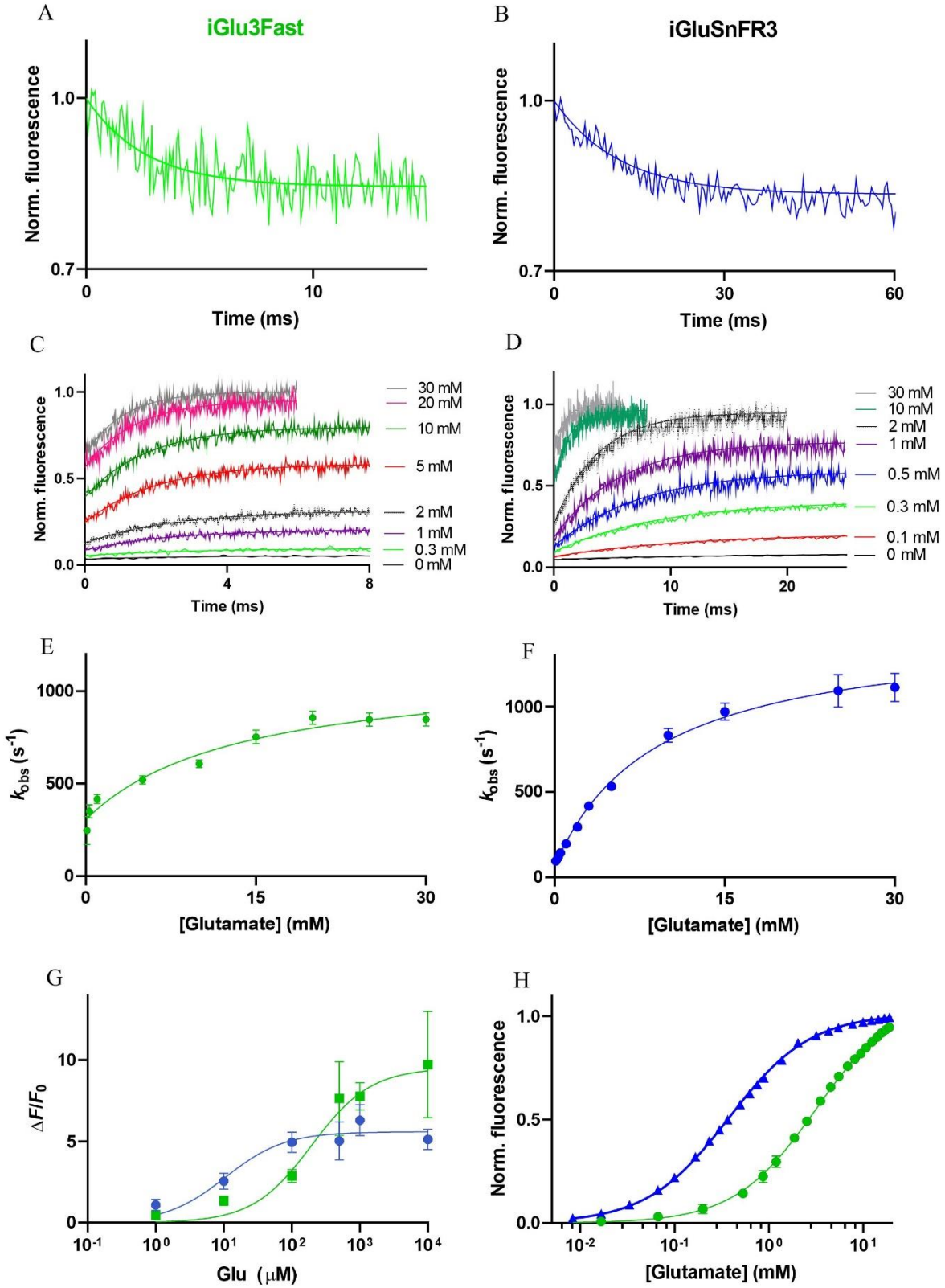
A
iGlu3Fast
Norm. fluorescence
1.0
0.7
0
10
Time (ms)
B
iGluSnFR3
Norm. fluorescence
1.0
0.7
0
30
60
Time (ms)
C
Norm. fluorescence
1.0
0.5
0.0
0
4
8
Time (ms)
30 mM
20 mM
10 mM
5 mM
2 mM
1 mM
0.3 mM
0 mM
D
Norm. fluorescence
1.0
0.5
0.0
0
10
20
Time (ms)
30 mM
10 mM
2 mM
1 mM
0.5 mM
0.3 mM
0.1 mM
0 mM
E
k_{obs} (s^{-1})
1000
500
0
0
15
30
[Glutamate] (mM)
F
k_{obs} (s^{-1})
1000
500
0
0
15
30
[Glutamate] (mM)
G
$\Delta F/F_0$
10
5
0
10^{-1}
10^{0}
10^{1}
10^{2}
10^{3}
10^{4}
Glu (μM)
H
Norm. fluorescence
1.0
0.5
0.0
10^{-2}
10^{-1}
10^{0}
10^{1}
[Glutamate] (mM)

Figure 4. **pH dependence**

A

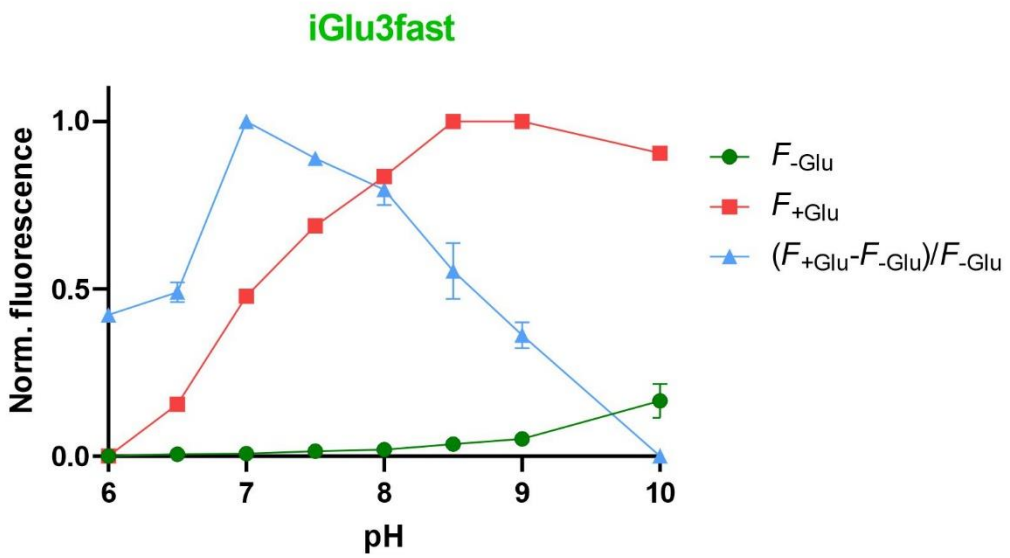

B

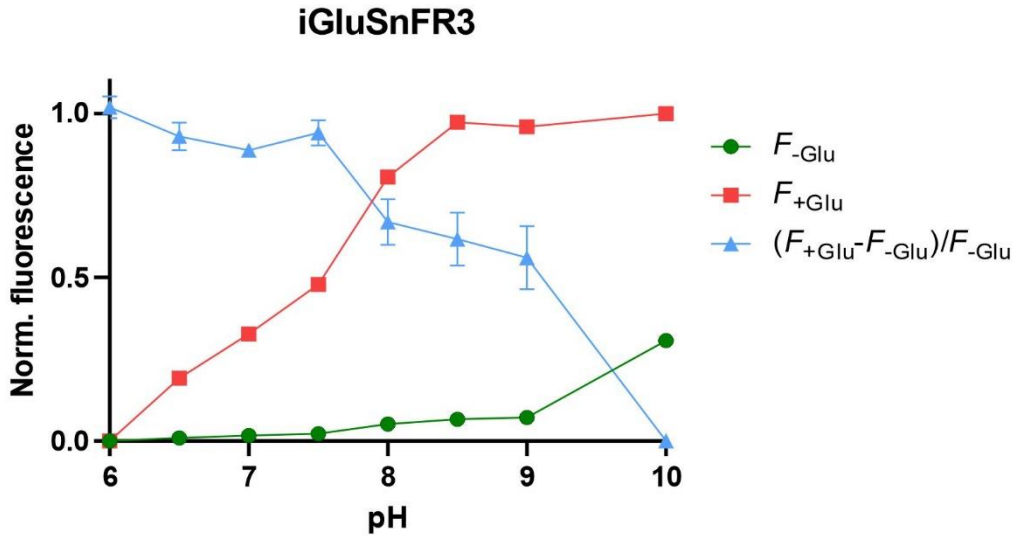

Figure 5. Ligand selectivity

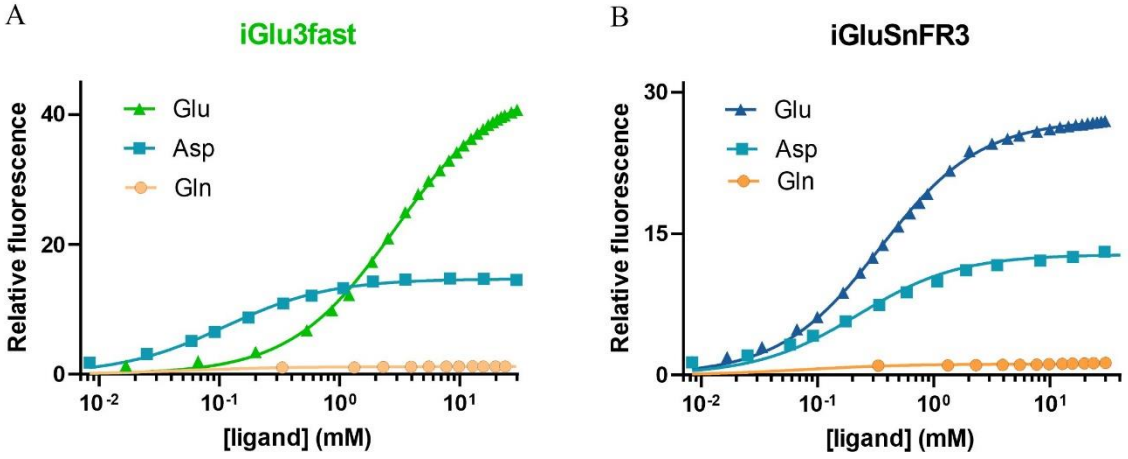

References

1. Marvin, J. S., Borghuis, B. G., Tian, L., Cichon, J., Harnett, M. T., Akerboom, J., Gordus, A., Renninger, S. L., Chen, T. W., Bargmann, C. I., Orger, M. B., Schreiter, E. R., Demb, J. B., Gan, W. B., Hires, S. A., and Looger, L. L. (2013) An optimized fluorescent probe for visualizing glutamate neurotransmission. *Nat Methods* **10**, 162-170

2. Helassa, N., Durst, C. D., Coates, C., Kerruth, S., Arif, U., Schulze, C., Wiegert, J. S., Geeves, M., Oertner, T. G., and Torok, K. (2018) Ultrafast glutamate sensors resolve high-frequency release at Schaffer collateral synapses. *Proc Natl Acad Sci U S A* **115**, 5594-5599

3. Dvorzhak, A., Helassa, N., Torok, K., Schmitz, D., and Grantyn, R. (2019) Single Synapse Indicators of Impaired Glutamate Clearance Derived from Fast iGlu u Imaging of Cortical Afferents in the Striatum of Normal and Huntington (Q175) Mice. *J Neurosci* **39**, 3970-3982

4. Coates, C., Kerruth, S., Helassa, N., and Torok, K. (2020) Kinetic Mechanisms of Fast Glutamate Sensing by Fluorescent Protein Probes. *Biophys J* **118**, 117-127

5. Aggarwal A, Liu R, Chen Y, Ralowicz AJ, Bergerson SJ, Tomaska F, Mohar B, Hanson TL, Hasseman JP, Reep D, Tsegaye G, Yao P, Ji X, Kloos M, Walpita D, Patel R, Mohr MA, Tillberg PW, Looger LL, Marvin JS, Hoppa MB, Konnerth A, Kleinfeld D, Schreiter ER, Podgorski K. (2023) Glutamate indicators with improved activation kinetics and localization for imaging synaptic transmission. *Nat Methods* **20**, 925-934

6. Chen, T-W., Wardill, T.J., Sun, Y., Pulver, S.R., Renninger, S.L., Baohan, A., Schreiter E.R., Kerr, R.A., Orger M.B., Jayaraman, V., Looger, L.L., Svoboda, K. and Kim, D.S. (2013) Ultrasensitive fluorescent proteins for imaging neuronal activity. *Nature* **499**, 295-300

7. Plested A. J, Mayer, M. L. (2009) Engineering a high-affinity allosteric binding site for divalent cations in kainate receptors. *Neuropharmacology* **56**, 114-20

8. Hao, Y., Toulmé, E., König, B., Rosenmund, C. and Plested A.J.R. (2023) Targeted sensors for glutamatergic neurotransmission. *Elife* **12**:e84029

9 Edelstein, A. D.,Tsichida, M. A., Amodaj, N., Pinkard, H., Vale, R. D. and Stuurman, N. (2014) Advanced methods of micriscope control using μManager software. *J. Biol. Methods* **1**(2):e10

10. Schindelin J, Arganda-Carreras I, Frise E, Kaynig V, Longair M, Pietzsch T, Preibisch S, Rueden C, Saalfeld S, Schmid B, Tinevez JY, White DJ, Hartenstein V, Eliceiri K, Tomancak P, Cardona A. (2012) Fiji: an open-source platform for biological-image analysis. *Nat Methods* **9**, 676-82

Supplementary data

Supplementary Table 1. Kinetic parameters of iGluSnFR3 and variants

Variant	F_{rel}	K_d mM	k_{-2} s^{-1}	K_1 M^{-1}	k_{+2} s^{-1}	K_d (calc) μM
iGlu3slow1	16 ± 1	0.058 ± 0.001	[a]0.017 ± 0.0001	0.121 ± 0.007	1260 ± 34	115
iGlu3slow2	23 ± 1	0.204 ± 0.008	[a]0.023 ± 0.0003	0.057 ± 0.014	1485 ± 222	272
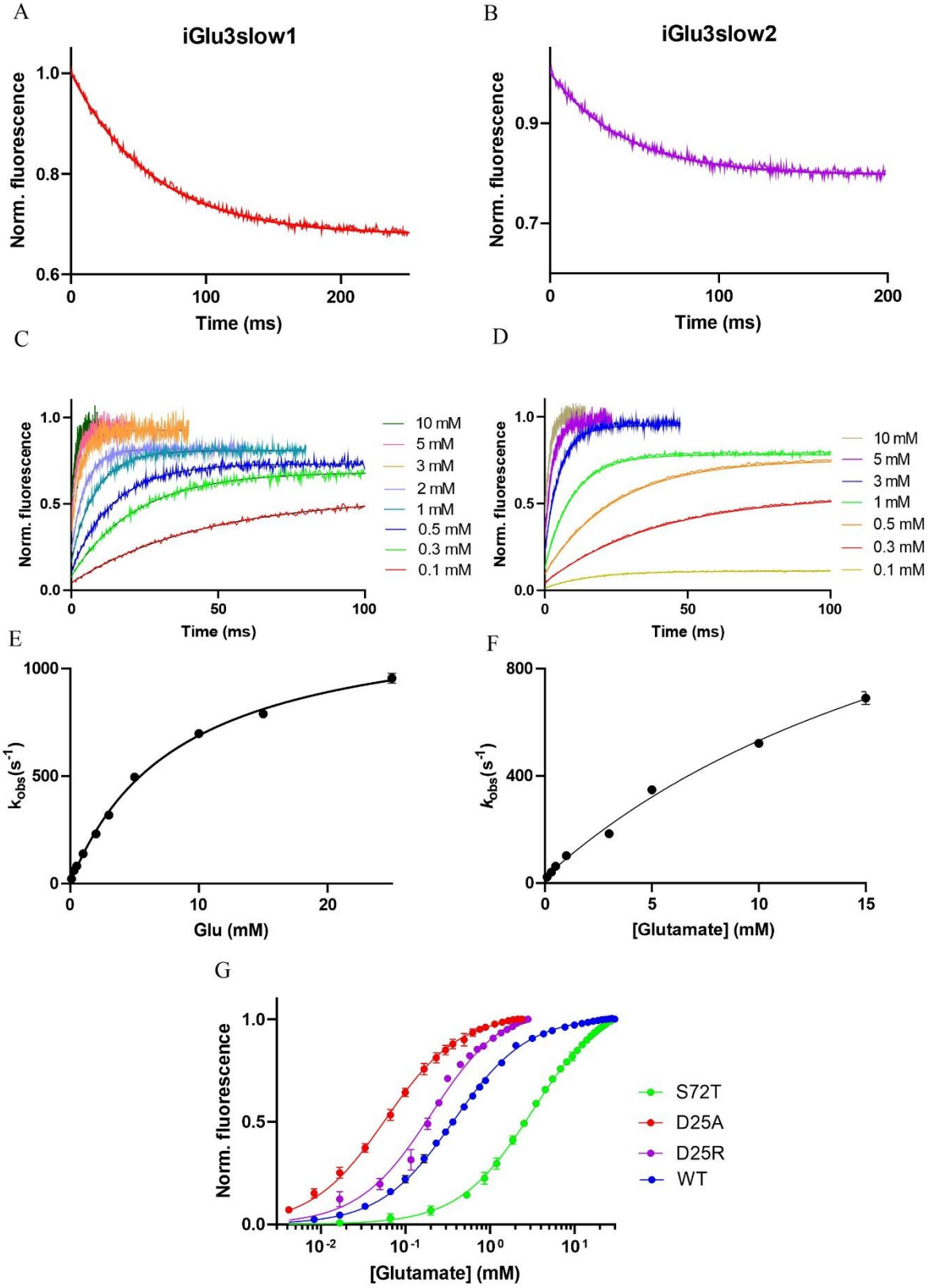
Supplementary Figure 1. Super-slow decay iGluSnFR3 variants